Three-dimensional Transesophageal Echocardiography for Transcatheter Patent Foramen Ovale Closure: Standardizing Anatomic Nomenclature and Novel Sizing Concepts

Tanuka Datta, MD, Nicholas Ruggiero, MD, Andrew Peters, MD, Ashley Pender, MD, Alec Vishnevsky, MD, and Praveen Mehrotra, MD, *Philadelphia, Pennsylvania*

INTRODUCTION

In patients amenable to transcatheter patent foramen ovale (PFO) closure, proper defect sizing and appropriate device size selection are imperative to ensure successful procedural outcomes and prevent recurrent strokes. However, PFO device sizing is currently highly variable, with multiple methods being utilized in clinical practice.[1] Nomenclature for describing PFO size remains unstandardized and continues to be based primarily on two-dimensional (2D) imaging despite our improved understanding of PFO morphology from three-dimensional (3D) transesophageal echocardiography (TEE; 3D-TEE).[2,3] Furthermore, residual right-to-left shunting remains as high as 25% and is associated with a 3-fold higher risk of recurrent stroke or transient ischemic attack after transcatheter PFO closure.[4-6] With the increasing number and types of devices being utilized for PFO closure,[5-7] standardized terminology and imaging techniques are necessary to ensure proper assessment of PFO size in clinical practice and trials, facilitate communication between cardiovascular specialists, and ensure optimal clinical outcomes. In this case report, we introduce standardized anatomic definitions for PFO dimensions and novel concepts for PFO sizing based on 3D-TEE for improved device size selection, which should be utilized during the preprocedural or intraprocedural imaging assessment for transcatheter PFO closure.

CASE PRESENTATION 1

A 66-year-old woman with a history of hypertension and breast cancer presented to our institution with slurred speech and headache. The patient was diagnosed with cryptogenic stroke after magnetic resonance imaging of the brain demonstrated acute right cerebellar infarction and computed tomography angiogram of the head and neck showed no large vessel occlusion. Lower extremity venous ultrasound and magnetic resonance venogram of the abdomen and pelvis demonstrated no evidence of deep venous thrombosis. A TEE was performed and demonstrated a "large" PFO and atrial septal aneurysm (ASA) with bidirectional shunting by color Doppler. The patient underwent implantation of a loop recorder, which did not demonstrate occult atrial fibrillation after 6 months of monitoring, and was subsequently referred for PFO closure.

Transcatheter PFO closure was performed with intraprocedural 3D-TEE, which demonstrated a 10-mm PFO tunnel length and a 7-mm tunnel height or separation between the septum primum and secundum (Figure 1A). However, the PFO tunnel width, that is, the size of the opening as seen with en face 3D volumetric and multiplanar imaging at both the left (LA) and right atrial (RA) openings, was much larger at 22 mm (Figure 1B–I, Videos 1 and 2). Based on the latter measurements, a 35-mm PFO occluder device was chosen, advanced across the defect, and deployed. After deployment, the device appeared well seated along the interatrial septum with no impingement on surrounding structures (Figure 2A–E, Video 3) or evidence of shunting by color Doppler or with agitated saline injection. There were no procedural complications. No residual right-to-left shunting was observed on the 1-month follow-up transthoracic echocardiogram.

CASE PRESENTATION 2

A 49-year-old man with history of hyperlipidemia and hypertension presented to our institution after awaking with aphasia and right hemiparesis. The patient received tPA and underwent mechanical thrombectomy for left middle cerebral artery stroke confirmed by brain magnetic resonance imaging. A TEE was subsequently performed that demonstrated a PFO with an ASA. After discharge, the patient underwent additional workup including hypercoagulable testing, which was unrevealing. A loop recorder did not reveal occult atrial fibrillation after 6 months of monitoring, and the patient was referred for transcatheter PFO closure, which was performed with TEE guidance.

Initial 3D-TEE imaging demonstrated a rightward displaced interatrial septum (Figure 3A–C, Video 4). With separation of the septum primum and secundum during a transient increase in RA pressure, the tunnel length was 2 mm, tunnel height was 2 to 3 mm, and tunnel width was 15 mm by 3D multiplanar imaging (Figure 3D–F). Given the short tunnel length, RA and LA PFO tunnel widths were identical. Based on the initial 15-mm tunnel width measurement, a 25-mm cclude device was chosen to close the PFO. A wire was then passed

From the Division of Cardiology, Thomas Jefferson University Hospital, Thomas Jefferson University, Sidney Kimmel Medical College, Philadelphia, Pennsylvania.
Keywords: Patent foramen ovale, Three-dimensional, Transesophageal echocardiography, Transcatheter closure
Correspondence: Praveen Mehrotra, MD, Associate Professor of Medicine, Division of Cardiology, Sidney Kimmel Medical College, Thomas Jefferson University, 925 Chestnut Street, Mezzanine Level, Philadelphia, PA 19107 (E-mail: *praveen.mehrotra@jefferson.edu*).

2468-6441
https://doi.org/10.1016/j.case.2022.10.007

VIDEO HIGHLIGHTS

Video 1: Case 1: 3D-TEE rendering and multiplanar images of PFO obtained from bicaval view. The PFO tunnel length is seen in 3D rendering *(top left)* and can be measured in the corresponding multiplanar image *(top right)*. The transverse plane is placed at RA opening *(top)* allowing for measurement of PFO tunnel width in the orthogonal view *(bottom left)*. En face multiplanar view of the interatrial septum with plane aligned in the direction of the PFO is shown in the *bottom right*.

Video 2: Case 1: En face 3D-TEE rendering of PFO as seen from the left atrium allowing for appreciation of large PFO tunnel width *(right)*. The SVC and aorta are seen in the foreground. The transverse plane is placed at the LA opening in bicaval multiplanar image *(top left)* allowing for appreciation of PFO tunnel width in orthogonal view *(bottom left)*.

Video 3: Case 1: 2D-TEE midesophageal 45° view demonstrating final positioning of 35-mm PFO occluder device.

Video 4: Case 2: 3D-TEE rendering and multiplanar images of PFO obtained from bicaval view. Tunnel length cannot be easily appreciated due to rightward displacement of interatrial septum but appears small during transient leftward displacement *(top left and right)*. The transverse plane is placed at tunnel opening *(top)*, demonstrating minimal separation between septum primum and septum secundum *(bottom left)*, precluding accurate measurement of PFO dimensions. En face multiplanar view of the interatrial septum with plane aligned in the direction of the PFO is shown in the *bottom right*.

Video 5: Case 2: 3D-TEE rendering and multiplanar images of PFO during wire sizing at the time of transcatheter PFO closure. The transverse plane is placed at tunnel opening *(top)* with wire causing mechanical separation of septum primum and septum secundum allowing for measurement of PFO tunnel width *(bottom left)*. En face multiplanar view of the interatrial septum with plane aligned in the direction of the PFO is shown in the *bottom right*.

Video 6: Case 2: Biplane 2D-TEE modified bicaval view demonstrating unsuccessful deployment of 25 mm PFO occluder device. The occluder device is unable to cover the tunnel and recoils posteriorly in the atria.

Video 7: Case 2: 2D-TEE midesophageal 45° view demonstrating final positioning of 35-mm PFO occluder device.

View the video content online at www.cvcasejournal.com.

across the PFO, resulting in improved visualization of the tunnel due to increased separation between the septum primum and secundum. With the wire tenting open in the tunnel, the PFO tunnel width was remeasured at 20 mm (Figure 3G–I, Video 5), while tunnel length was unchanged. Despite the larger PFO tunnel width, the chosen device size was not changed due to the concern for the very short tunnel length of 2 mm. The 25-mm occluder device, however, failed to seat well along the interatrial septum (Figure 4A, Video 6) after initial deployment, and the device was recaptured and removed. A 35-mm PFO occluder device was then advanced across the PFO and deployed. After deployment, the device appeared well seated along the interatrial septum with no impingement on surrounding structures (Figure 4B–D, Video 7) or evidence of shunting by color Doppler or with agitated saline injection. There were no procedural complications. No residual right-to-left shunting was observed on the 1-month follow-up transthoracic echocardiogram.

DISCUSSION

PFO Morphology

The PFO is a tunnel formed by the flap-like, thin septum primum and thicker septum secundum in the anterosuperior portion of the interatrial septum.[8] The LA opening is adjacent to the aorta and superior vena cava and is typically crescentic in shape.[9] However, PFO anatomy can be highly variable, with different sizes and degrees of physiological significance. Although in normal physiologic conditions the left-to-right atrial pressure differential keeps the tunnel closed and prevents communication between the 2 atria, right-to-left shunting can occur due to conditions that increase right-sided pressure, while some patients exhibit intermittent or continuous left-to-right shunting.

Standard Terminology for PFO Dimensions

Proposed standard terminology for PFO dimensions with important imaging considerations are shown in Table 1. Techniques for measurement of PFO tunnel length, height, and width with 3D-TEE are depicted in Figure 1. PFO tunnel "length" is an established term that describes the distance between the RA opening at the fossa ovalis and the LA opening of the PFO.[8-10] We recommend that the term PFO tunnel "height" be used to describe the separation between the septum primum and septum secundum (i.e., the minor axis of the oval opening), although both "width" and "height" have been used interchangeably in the literature to describe this dimension.[1,7,12,13] We reserve the use of the term PFO tunnel "width" to describe the size of the RA or LA openings, which are only appreciated with en face PFO visualization (i.e., the major axis of the oval opening). The PFO tunnel width has only recently been emphasized in the literature[11] and is better suited to be measured with biplane or 3D multiplanar imaging rather than 2D imaging alone.[2,3,11] In addition to measurement of the PFO tunnel width, en face assessment of the PFO with 3D-TEE facilitates more accurate assessment of PFO tunnel length and height, may be useful in cases of variant PFO anatomy such as double orifice tunnels, and can aid in determining the adequacy of tunnel closure after device deployment.

Device Size Selection for PFO Closure

Currently, there is no one established technique for PFO device size selection.[1,10] Some operators and manufacturers recommend balloon sizing, which transforms the PFO tunnel from a slit-like, elliptical orifice to a circular defect in which the balloon waist diameter measured on angiography approximates the PFO tunnel width by 3D-TEE.[1] However, care must be taken not to overstretch the PFO or tear the intertrial septum with balloon inflation.[10] For the Amplatzer PFO occluder, the most recent instructions for use[14] recommend a multiparametric approach taking into account PFO tunnel length, the size of the ASA based on septal excursion, and the thickness of the septum secundum. In our experience as well as that of other authors,[3,11] the PFO tunnel width is a better

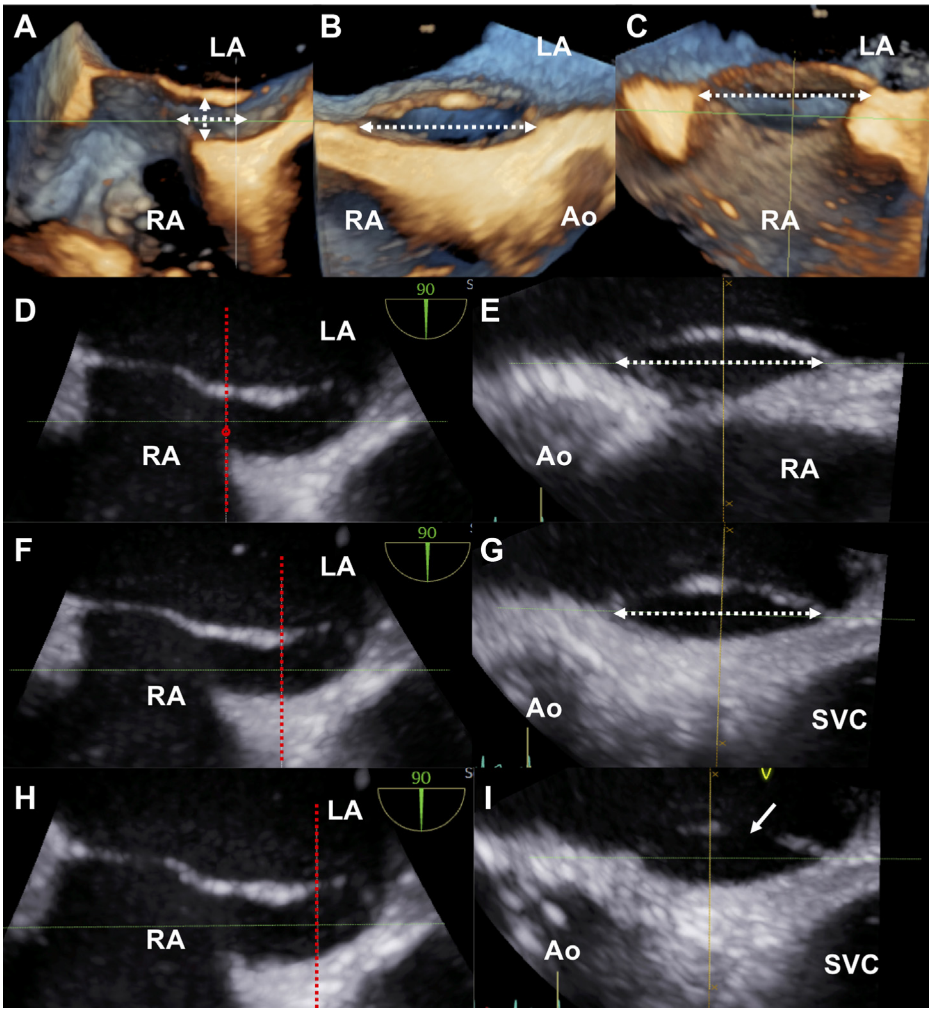

Figure 1 Case 1: Volumetric and multiplanar 3D-TEE images of PFO. **(A)** Three-dimensional rendering of bicaval view (90°) depicting PFO tunnel length *(horizontal dotted white arrow)* and tunnel height *(vertical dotted white arrow)*. **(B)** En face 3D rendering of PFO (orthogonal to bicaval view) as seen from LA depicting tunnel width *(dotted white arrow)* at LA opening. **(C)** En face 3D rendering of PFO as seen from RA (orthogonal to bicaval view) demonstrating tunnel width *(dotted white arrow)* at RA opening. **(D)** Bicaval 3D multiplanar image (90°) of PFO with transverse imaging plane *(dotted red line)* used to create orthogonal multiplanar view **(E)** for measurement of PFO tunnel width *(white arrow)* at RA opening. **(F)** Bicaval 3D multiplanar image (90°) of PFO with transverse imaging plane *(red dotted line)* advanced superiorly to create orthogonal multiplanar view **(G)** for measurement of PFO tunnel width *(white arrow)* at LA opening. **(H)** Bicaval 3D multiplanar image (90°) of PFO with further advancement of transverse imaging plane along apparent tunnel length demonstrates in orthogonal view **(I)** that the roof of the tunnel is no longer intact *(white arrow)* due to crescentic LA opening. *Ao*, Aorta; *LA*, Left atrium; *RA*, right atrium; *SVC*, superior vena cava.

descriptor of tunnel size and, therefore, may be a more ideal parameter for device size selection prior to transcatheter closure. A schematic demonstrating defect sizing and device size selection based on PFO tunnel width is shown in Figure 5. With this sizing technique, the diameter of the RA disk of the circular closure device must exceed the RA PFO tunnel width since the closure device will tend to "center" at the RA opening (Figure 2C–E). If the RA disk diameter is smaller than the RA PFO tunnel opening, thrombi could potentially enter the tunnel at the margins of the device. In addition to obtaining PFO dimensions, the anteroposterior dimensions of the atria should be measured in a midesophageal 45° view to ensure that the disk can be adequately accommodated (particularly for larger sized devices) without impingement on adjacent cardiac structures such as the posterior atrial wall or aortic sinuses.

Our 2 cases emphasize the importance of the PFO tunnel width measurement for device sizing and that a larger PFO tunnel width may necessitate a larger closure device despite a relatively smaller PFO tunnel length.[15] Based on the instructions for use,[14] a 25-mm PFO occluder device would have been recommended in both of our cases. In case 1, a 25-mm device would have left only 1.5 mm on either side of the tunnel width to cover the entire defect based on the 22-mm tunnel width measurement, while on the LA side, the disk size (18 mm) would have been smaller than the tunnel width. In case 2, a 25-mm device did not seat well along the

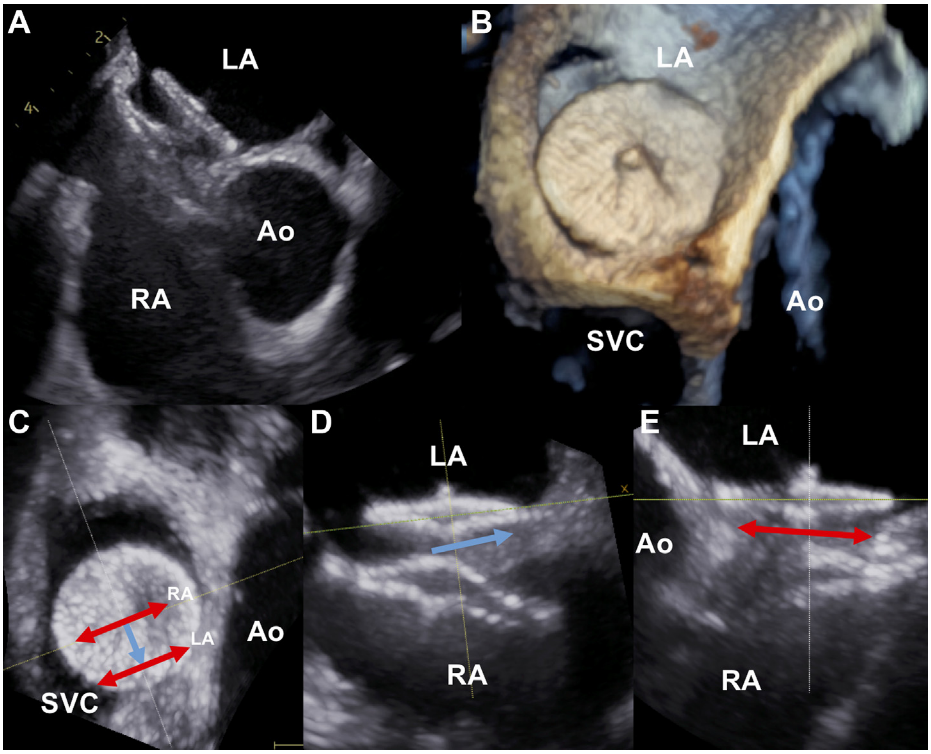

Figure 2 Case 1: 2D- and 3D-TEE images after transcatheter PFO closure. **(A)** Midesophageal 45° short-axis view showing deployment of PFO occluder device along interatrial septum. **(B)** En face 3D rendering of LA disk of PFO occluder device in the anterosuperior portion of the interatrial septum. **(C)** En face 3D multiplanar view of LA disk with *red arrows* approximating location of PFO tunnel widths at RA and LA openings and *blue arrow* demonstrating tunnel length. **(D)** Bicaval 3D multiplanar view demonstrating PFO tunnel length *(blue arrow)* relative to PFO occluder device. The device is "centered" at the RA opening. **(E)** Three-dimensional multiplanar view (orthogonal to bicaval view) demonstrating PFO tunnel width at RA opening *(red arrow)* relative to PFO occluder device. The tunnel width has been adequately "sandwiched" by both RA and LA disks. *Ao*, Aorta; *LA*, left atrium; *RA*, right atrium; *SVC*, superior vena cava.

interatrial septum and could not cover the PFO due to the larger tunnel width of 20 mm. In both cases, the relatively smaller tunnel lengths belied the larger widths of both defects. Prior studies have shown that the PFO tunnel height correlates poorly with tunnel length and width.[1,3,11] In our experience, PFO tunnel length is also a poor predictor of tunnel width as illustrated in these 2 cases, thus indicating the importance of measuring all PFO dimensions prior to device size selection. Significant "oversizing" of the PFO tunnel width by the larger 35-mm PFO occluder device in both cases resulted in stable device seating and adequate device coverage of the PFO without impingement on surrounding structures despite relatively smaller tunnel lengths.

PFO "Wire Sizing"

Patent foramen ovale dimensions cannot be accurately measured in all cases due to the relatively higher LA pressure, which pushes the septum primum against the septum secundum, precluding accurate visualization of the tunnel. While imaging during transient increases in RA pressure such as simulated Valsalva or inspiration may briefly improve visualization of the PFO tunnel, this technique may still be inadequate to completely visualize and estimate the size of the PFO tunnel as demonstrated in case 2. In such cases, "wire sizing" should be strongly considered. In this technique, biplane and/or 3D-TEE imaging is performed at the time of transcatheter closure after introduction of a wire through the tunnel to induce mechanical separation of the septum primum from the secundum and allow for easier assessment of PFO dimensions.[11] In cases performed with TEE guidance at our institution, we routinely measure PFO dimensions before and after wire placement to ensure that initial PFO measurements are not underestimated due to incomplete tunnel visualization. In our second case, the minimal separation of the septum primum and secundum led to a significant underestimation of the PFO tunnel width. Wire sizing in this case led to a 33% increase in the PFO tunnel width measurement, which we believe was the reason for the improved seating of the larger 35-mm PFO occluder device. Three-dimensional intracardiac echocardiography could theoretically provide similar benefits for PFO sizing but may be limited due to the significantly smaller size of its volumetric acquisitions.

CONCLUSION

Our cases highlight the importance of standardizing anatomic nomenclature for PFOs and proper tunnel sizing with 3D-TEE for ensuring procedural success after transcatheter PFO closure. In particular, the PFO tunnel width is a key measurement, which may aid in the selection of the appropriate occluder device size. In our 2 cases, the presence of a large PFO tunnel width necessitated larger size devices to ensure adequate oversizing and complete tunnel closure, which were deployed safely despite

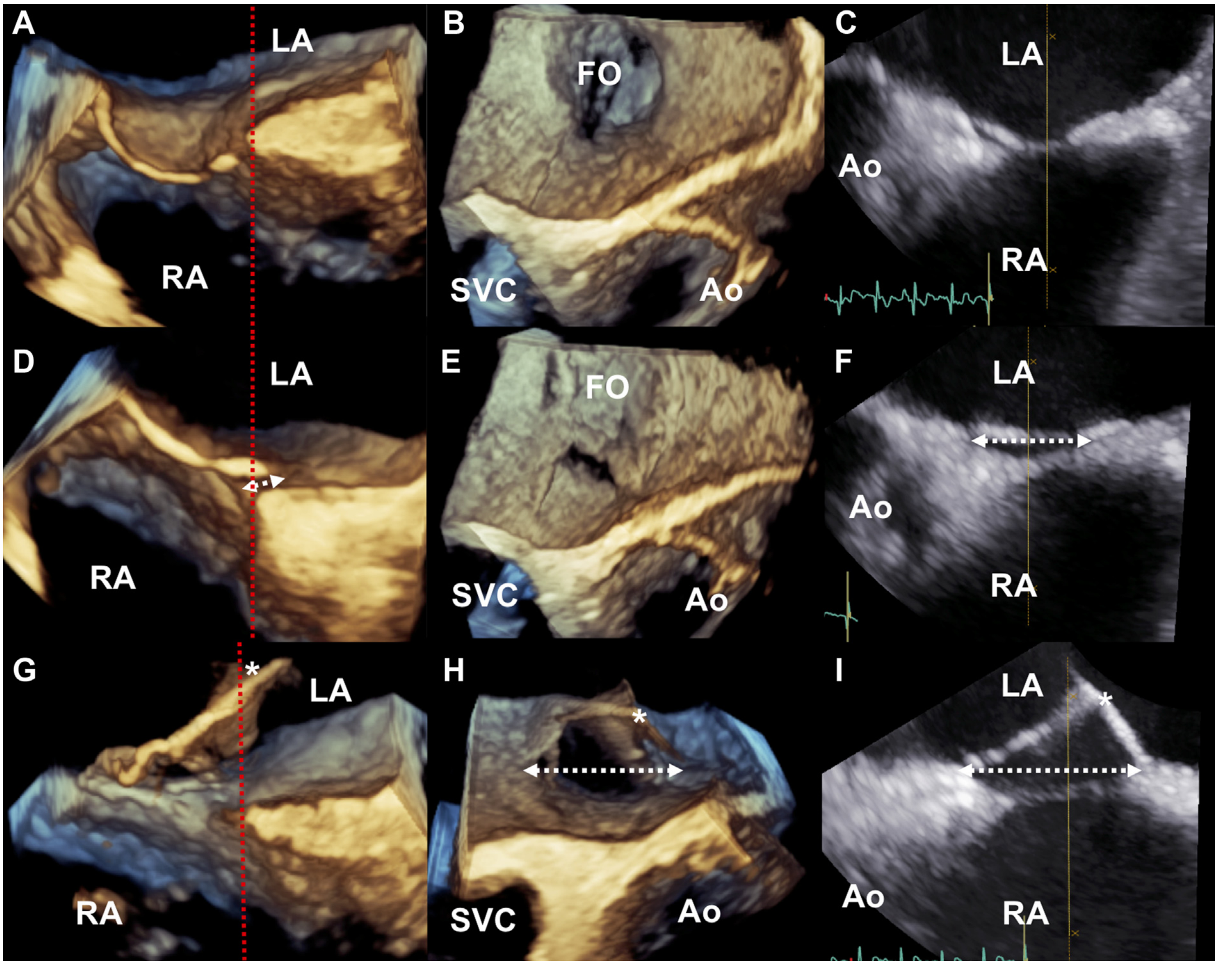

Figure 3 Case 2: Volumetric and multiplanar 3D-TEE images of PFO. Three-dimensional rendering of bicaval **(A)** and en face **(B)** view of PFO from the left atrium (LA) demonstrating ASA with septum primum displaced toward the right atrium precluding visualization of PFO tunnel and measurement of tunnel width in corresponding 3D multiplanar image **(C)**. Three-dimensional rendering of bicaval **(D)** and en face **(E)** view of PFO from the LA with septum primum lifted 2-3 mm off septum secundum due to transient increase in RA pressure. Three-dimensional bicaval view demonstrates very short tunnel length (2 mm, *dotted white arrow*). Three-dimensional en face view depicts crescentic opening of PFO into the LA and PFO tunnel width. In the corresponding 3D multiplanar image **(F)**, the PFO tunnel width *(dotted white arrow)* measures 15 mm. Three-dimensional rendering of bicaval **(G)** and en face **(H)** view of wire (*) through PFO ("wire sizing") allowing for easier measurement of PFO tunnel width (20 mm) by multiplanar 3D imaging **(I)** as shown with the larger *dotted white arrow*. Three-dimensional multiplanar views optimized to visualize PFO tunnel width (panels **C**, **F**, and **I**) are obtained from the plane orthogonal to the bicaval view *(dotted red lines)*. *Ao*, Aorta; *FO*, fossa ovalis; *RA*, right atrium; *SVC*, superior vena cava.

relatively smaller tunnel lengths. In cases of minimal separation between the septum primum and secundum, PFO wire sizing may provide improved tunnel visualization and potentially more accurate assessment of PFO dimensions. Further research is needed to determine the optimal degree of PFO tunnel width oversizing and whether a sizing strategy based on PFO tunnel width results in improved procedural success and clinical outcomes.

ETHICS STATEMENT

The authors declare that the work described has been carried out in accordance with The Code of Ethics of the World Medical Association (Declaration of Helsinki) for experiments involving humans.

CONSENT STATEMENT

The authors declare that informed patient consent was not provided for the following reason: the authors declare that since this was a retrospective, observational imaging study utilizing deidentified data, informed consent was not required from the patient under an IRB exemption status.

FUNDING STATEMENT

The authors declare that this report did not receive any specific grant from funding agencies in the public, commercial, or not-for-profit sectors.

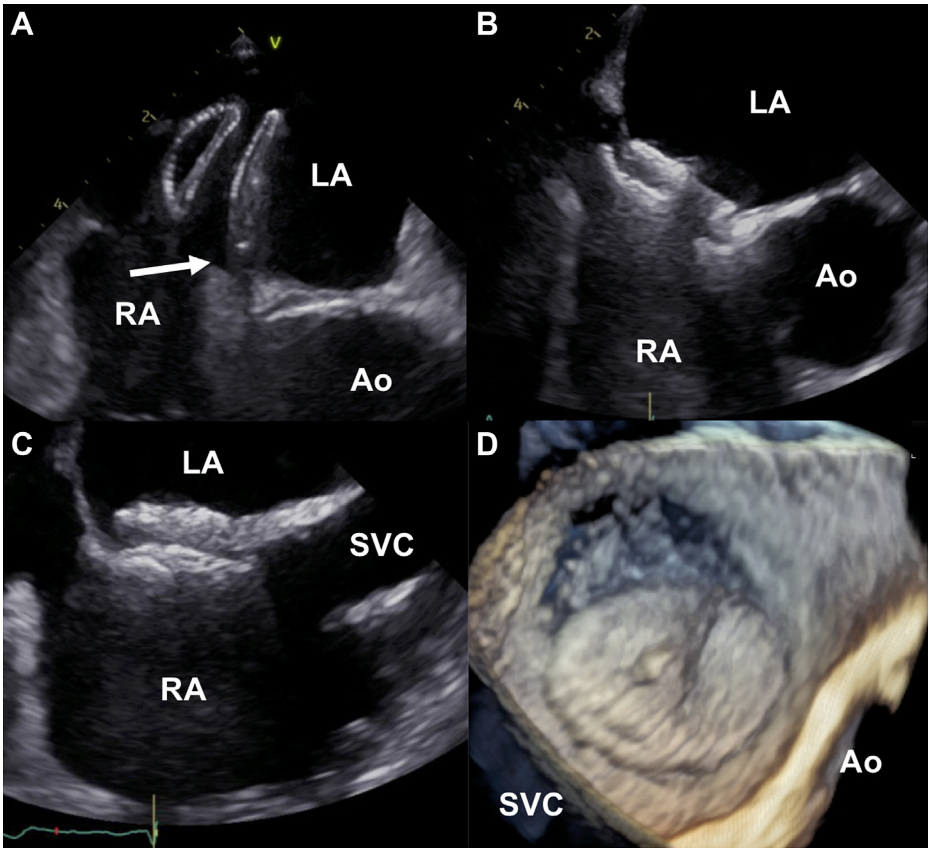

Figure 4 Case 2: 2D- and 3D-TEE images after transcatheter PFO closure. Midesophageal 45° view **(A)** demonstrating suboptimal deployment of 25-mm occluder. Due to its smaller size relative to the PFO width, the device did not capture the PFO *(white arrow)* at tunnel opening and easily recoiled posteriorly in the atria. Midesophageal 45° view **(B)**, bicaval view **(C),** and en face 3D rendering **(D)** from LA demonstrating improved seating of larger 35-mm PFO occluder device along interatrial septum. *Ao*, Aorta; *LA*, left atrium; *RA*, right atrium; *SVC*, superior vena cava.

Table 1 Proposed standardized terminology and definitions for PFO dimensions

PFO dimension	Definition	Important imaging considerations
Tunnel length	• Describes the distance between the RA opening at the fossa ovalis and the LA opening of the PFO	• Best visualized in the bicaval view[10] • A PFO tunnel length greater than 8-12 mm has been proposed as a cutoff for classifying a "long" tunnel PFO[2,10] • Due to the crescentic opening of the PFO in the left atrium, tunnel length may appear artificially longer on 2D-TEE images and may be more accurately depicted with 3D multiplanar imaging
Tunnel height	• Describes the separation between the septum primum and septum secundum • Represents the minor axis of the oval-shaped opening	• Dynamic measurement that depends on degree of septum primum excursion and changes in RA pressure • Varies with respiratory and cardiac cycle[3] • Variable depending on location (e.g., RA vs LA side) measured in the tunnel[3]
Tunnel width at LA or RA opening	• Describes the size of the opening of the PFO tunnel on the RA side at the fossa ovalis or on the LA side • Represents the major axis of the oval-shaped opening	• Better visualized with biplane or 3D-TEE[2,3,11] • Measurement is easier to make when there is separation of the septum primum from septum secundum • The PFO width at the LA opening is measured while the "roof" of the PFO is intact immediately before crescentic LA opening

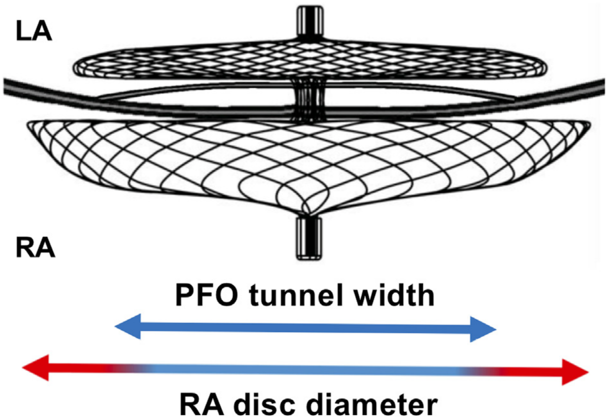

Figure 5 PFO sizing and device size selection schematic based on tunnel width for transcatheter PFO closure. When the PFO tunnel width at the RA opening is adequately oversized by the RA disk, the PFO tunnel will be sufficiently closed and prevent passage of thrombi from the right to left atrium. The *blue arrow* depicts PFO width at RA opening and the *multicolor arrow* depicts RA disk diameter with the *red portion* showing degree of PFO tunnel width oversizing. *LA*, Left atrium; *RA*, right atrium.

DISCLOSURE STATEMENT

P.M. has stock ownership in Abbott. The remaining authors have nothing to declare.

SUPPLEMENTARY DATA

Supplementary data to this article can be found online at https://doi.org/10.1016/j.case.2022.10.007.

REFERENCES

1. Kumar P, Rusheen J, Tobis JM. A comparison of methods to determine patent foramen ovale size. Catheter Cardiovasc Interv 2020;96:E621-9.
2. Rana BS, Shapiro LM, McCarthy KP, Ho SY. Three-dimensional imaging of the atrial septum and patent foramen ovale anatomy: Defining the morphological phenotypes of patent foramen ovale. Eur J Echocardiogr 2010;11:i19-25.
3. Tanaka J, Izumo M, Fukuoka Y, Saitoh T, Harada K, Harada K, et al. Comparison of two-dimensional versus real-time three-dimensional transesophageal echocardiography for evaluation of patent foramen ovale morphology. Am J Cardiol 2013;111:1052-6.
4. Deng W, Yin S, McMullin D, Inglessis-Azuaje I, Elmariah S, Hung J, et al. Residual shunt after patent foramen ovale closure and long-term stroke recurrence: a prospective cohort study. Ann Intern Med 2020;172:717-25.
5. Mas JL, Derumeaux G, Guillon B, Massardier E, Hosseini H, Mechtouff L, et al. Patent foramen ovale closure or anticoagulation vs. Antiplatelets after stroke. N Engl J Med 2017;377:1011-21.
6. Søndergaard L, Kasner SE, Rhodes JF, Andersen G, Iversen HK, Nielsen-Kudsk JE, et al. Patent foramen ovale closure or antiplatelet therapy for cryptogenic stroke. N Engl J Med 2017;377:1033-42.
7. Gaspardone A, Sgueglia GA, de Santis A, D'Ascoli E, Iamele M, Piccioni F, et al. Predictors of residual right-to-left shunt after percutaneous suture-mediated patent fossa ovalis closure. JACC Cardiovasc Interv 2020;13:2112-20.
8. Silvestry FE, Cohen MS, Armsby LB, Burkule NJ, Fleishman CE, Hijazi ZM, et al. Guidelines for the echocardiographic assessment of atrial septal defect and patent foramen ovale: from the American society of echocardiography and society for cardiac angiography and interventions. J Am Soc Echocardiogr 2015;28:910-58.
9. Kutty S, Sengupta PP, Khandheria BK. Patent foramen ovale: the known and the to be known. J Am Coll Cardiol 2012;59:1665-71.
10. Collado FMS, Poulin MF, Murphy JJ, Jneid H, Kavinsky CJ. Patent foramen ovale closure for stroke prevention and other disorders. J Am Heart Assoc 2018;7:1-22.
11. Demulier L, Paelinck BP, Coomans I, Hemelsoet D, de Backer J, Campens L, et al. A new dimension in patent foramen ovale size estimation. Echocardiography 2020;37:1049-55.
12. Akhondi A, Gevorgyan R, Tseng CH, Slavin L, Dao C, Liebeskind DS, et al. The association of patent foramen ovale morphology and stroke size in patients with paradoxical embolism. Circ Cardiovasc Interv 2010;3:506-10.
13. Hołda MK, Koziej M. Morphometric Features of Patent Foramen Ovale as a Risk Factor of Cerebrovascular Accidents: A Systematic Review and Meta-Analysis. Cerebrovasc Dis 2020;49:1-9.
14. Abbott Laboratories. Amplatzer Talisman PFO Occluder Instructions for Use [Internet]. 2021 [cited 2022 May 9]. Available from: https://www.cardiovascular.abbott/us/en/hcp/manuals-and-technical-resources.html. Accessed May 9, 2022.
15. Rana BS, Thomas MR, Calvert PA, Monaghan MJ, Hildick-Smith D. Echocardiographic evaluation of patent foramen ovale prior to device closure. JACC Cardiovasc Imaging 2010;3:749-60.